HYBRIDIZING RAVIART-THOMAS ELEMENTS FOR THE HELMHOLTZ EQUATION

PETER MONK, JOACHIM SCHÖBERL, ASTRID SINWEL

Abstract. This paper deals with the application of hybridized mixed methods for discretizing the Helmholtz problem. Starting from a mixed formulation, where the flux is considered a separate unknown, we use Raviart-Thomas finite elements to approximate the solution. We present two ways of hybridizing the problem, which means breaking the normal continuity of the fluxes and then imposing continuity weakly via functions supported on the element faces or edges. The first method is the Ultra-Weak Variational Formulation, first introduced by Cessenat and Després [7]; the second one uses Lagrange multipliers on element interfaces. We compare the two methods, and give numerical results. We observe that the iterative solvers applied to the two methods behave well for large wave numbers.

1. Introduction

If we wish to solve the Helmholtz equation with a large wave number κ (see (1) for the definition of this parameter) using an h-version finite element scheme in $\mathbb{R}^d$, $d = 2, 3$, the dimension of the linear system must grow faster than $O(\kappa^d)$ to maintain accuracy because of pollution error (see [19]). Thus we have to solve a large sparse and indefinite matrix problem. Standard iterative solution techniques usually perform more poorly as κ increases (for example, using a standard multigrid scheme, the coarsest grid has a mesh size of the order $O(1/\kappa)$). Although more exotic multigrid schemes have been applied [12], they also require more iterations at higher wave numbers. In this paper we will investigate hybridized Raviart-Thomas methods for the Helmholtz equation with a view to obtaining linear systems that can be solved more efficiently. In numerical experiments, we observe that the appropriate iterative solver converges in a number of iterations that is bounded independent of κ.

To formulate a model Helmholtz equation, let $\Omega \subset \mathbb{R}^d$, $d = 2, 3$ be a bounded domain with boundary $\Gamma = \partial\Omega$, which is assumed to be a Lipschitz polyhedron (polygon in two dimensions) that can be covered by tetrahedral elements in three dimensions (or triangles in two dimensions). By n we denote the unit outward

Date: July 28, 2008.

The research of the first author was supported in part by the U.S. Air Force Office of Scientific Research under Grant FA9550-05-1-0127. The last author acknowledge support from the Austrian Science Foundation FWF within project grant Start Y-192, "hp-FEM: Fast Solvers and Adaptivity".

normal. We consider the following boundary value problem for the scalar field $u : \Omega \to \mathbb{C}$

$$
\begin{aligned}
\Delta u + \kappa^2 u &= 0 && \text{in } \Omega, \\
\frac{1}{i\kappa}\frac{\partial u}{\partial n} - \eta u &= Q\left[\frac{1}{i\kappa}\frac{\partial u}{\partial n} + \eta u\right] + g && \text{on } \Gamma.
\end{aligned} \tag{1}
$$

We assume that the wave number κ is a real parameter. On the boundary, $\eta \in L^\infty(\Gamma)$ is a real valued, uniformly bounded and strictly positive function, Q is real valued and piecewise constant with $|Q| \leq 1$, and $g \in L^2(\Gamma)$ is the given, possibly complex valued, boundary data. Provided $Q \neq 1$ we may rewrite this boundary condition as

$$
\frac{\partial u}{\partial n} - i\kappa\frac{1+Q}{1-Q}\eta u = \frac{i\kappa}{1-Q}g.
$$

This shows that the second equation in (1) is a standard impedance boundary condition as long as $Q \neq 1$. For special choices of Q, we obtain Dirichlet, Neumann and absorbing boundary conditions:

- $Q = 1$: Dirichlet, $u = -\frac{1}{2\eta}g$,
- $Q = -1$: Neumann, $\frac{1}{i\kappa}\frac{\partial u}{\partial n} = g/2$,
- $Q = 0$: absorbing, $\frac{1}{i\kappa}\frac{\partial u}{\partial n} - \eta u = g$.

The solution of problem (1) can be approximated using a mixed method with the standard Raviart-Thomas finite element space for the fluxes, and a discontinuous space for the scalar field. The hybrid methods we shall examine are modifications of this scheme. By hybridization, we mean that we break all continuity assumptions on the fluxes, and then reimpose them via new unknowns associated with facets or edges between elements. We derive two different methods to reenforce the required continuity. One method is motivated by the Ultra Weak Variational Formulation (UWVF) of the Helmholtz equation [7, 8, 11], but using mixed finite element spaces. The second method is a more direct hybridization similar to those already developed for Laplace's equation [2, 5, 9]. For our second method, we propose to use a preconditioned conjugate gradient (CG) method to solve the resulting complex-symmetric problem. We observe good behavior of the preconditioner with respect to the wave number and the polynomial degree of the finite element space.

Another reason for studying the UWVF hybridized Raviart-Thomas scheme is that it can then be seamlessly coupled to a standard UWVF that uses plane wave ansatz functions element by element. This allows the use of standard finite elements on small elements and plane waves on larger elements and is useful, for example, when geometric mesh refinement towards singularities of the solution is used. Large, plane-wave elements can be used away from the singularity, whereas polynomial finite elements may be better suited in the vicinity of the singularity.

Thereby, one can improve convergence around the singularity, while serious ill-conditioning of the system matrix is avoided. We present some numerical results for a combined method later in the paper.

We should note that there are many other ways to use discontinuous basis functions, and to hybridize the methods. An important paper on plane wave based discontinuous Galerkin methods (of which the UWVF is a special case, but outside the theoretical analysis) can be found in [16]. Coupling of plane wave and polynomial based methods is possible in the framework of that paper. Other methods that can couple plane wave and polynomial basis functions include the partition of unity finite element method [3, 23], and the discontinuous enrichment approach [13, 14].

Throughout the following, for a complex quantity $z \in \mathbb{C}$, let $\overline{z}$ denote its complex conjugate. For any Hilbert space X, let $\langle \cdot, \cdot \rangle_X$ denote its inner product and $\| \cdot \|_X$ be the corresponding norm. For a linear operator $F : X \to X$, its adjoint is denoted by F^*. For a domain A, let $L^2(A)$ be the complex Lebesgue space. It is equipped with the complex inner product $\langle u, v \rangle_{L^2(A)} := (u, v)_A := \int_A u\overline{v}\, dx$ and the induced norm $\|u\|_{L^2(A)} = \|u\|_A$. By $H^1(A)$ we denote the standard, complex valued Sobolev space of weakly differentiable functions. Let $H^{1/2}(\partial A)$ be its trace space. Moreover, we need the space of functions with weak divergence

$$H(\mathrm{div}; A) := \{\sigma \in [L^2(A)]^d : \mathrm{div}\, \sigma \in L^2(A)\},$$

and for suitably smooth domains

$$H_0(\mathrm{div}; A) := \{\sigma \in [L^2(A)]^d \ : \ \mathrm{div}\, \sigma \in L^2(A),\ \sigma \cdot n = 0 \text{ on } \partial A\}.$$

The remainder of this paper is organized as follows: In Section 2, a mixed variational formulation of the Helmholtz problem is stated. Existence and uniqueness for the mixed system are verified, and a standard method using Raviart-Thomas finite elements is applied. We also describe the continuous UWVF. In Section 3, the polynomial UWVF and the facet-based hybridization method are introduced, and are shown to be equivalent to the original Raviart-Thomas method. A comparison shows that the two methods are related by a change of variables. In Section 4, iterative methods for the solution of the respective systems of equations are proposed. Finally, numerical tests are presented in Section 5.

2. Variational methods for the Helmholtz problem

In this section we shall recall two variational methods for approximating the solution of (1). First we outline a standard mixed approach using Raviart-Thomas elements. Then we recall the UWVF.

2.1. **A mixed method based on Raviart-Thomas elements.**

We now recall a standard mixed formulation of the Helmholtz equation suitable for discretization by Raviart-Thomas elements. We want to find the scalar field u and the

vector-valued flux field $\boldsymbol{v} = -\frac{1}{i\kappa}\nabla u$. We denote the Neumann trace, which is the normal component of the flux vector $\boldsymbol{v}$, by $\boldsymbol{v}_n := \boldsymbol{v} \cdot n$ on Γ.

Since we are using a standard mixed method, the Neumann boundary conditions is a special case since it is essential and needs to be enforced on the trial and test spaces. Therefore we assume that $-1 < Q \leq 1$ ruling out this case.

Then the boundary value problem for the Helmholtz equation (1) can be written in mixed form as

$$\begin{aligned} -i\kappa u &= \operatorname{div} \boldsymbol{v} \quad \text{in } \Omega, \\ -i\kappa \boldsymbol{v} &= \nabla u \quad \text{in } \Omega, \\ -\boldsymbol{v}_n - \eta u &= Q[-\boldsymbol{v}_n + \eta u] + g \quad \text{on } \Gamma. \end{aligned} \tag{2}$$

For the variational formulation of this problem we need the following spaces

$$U = L^2(\Omega) \text{ and } V = \left\{ \boldsymbol{v} \in H(\operatorname{div}; \Omega) \mid \boldsymbol{v}_n \in L^2(\Gamma) \right\}$$

where the norm on V is given by

$$\|\boldsymbol{v}\|_V^2 = \|\nabla \cdot \boldsymbol{v}\|_{L^2(\Omega)}^2 + \|\boldsymbol{v}\|_{L^2(\Omega)}^2 + \|\boldsymbol{v}_n\|_{L^2(\Gamma)}^2.$$

The weak solution $(u, \boldsymbol{v}) \in U \times V$ satisfies

$$\begin{aligned} (i\kappa u, \xi)_\Omega + (\operatorname{div} \boldsymbol{v}, \xi)_\Omega &= 0 && \forall \xi \in U, \\ -(u, \operatorname{div} \boldsymbol{\tau})_\Omega + (i\kappa \boldsymbol{v}, \boldsymbol{\tau})_\Omega - (\tfrac{q}{\eta}\boldsymbol{v}_n, \boldsymbol{\tau}_n)_{\partial\Omega} &= (\tfrac{1}{\eta(1+Q)} g, \boldsymbol{\tau}_n)_{\partial\Omega} && \forall \boldsymbol{\tau} \in V, \end{aligned} \tag{3}$$

where $q = \frac{1-Q}{1+Q}$.

Lemma 1. *Suppose Ω is a Lipschitz domain. For $g \in L^2(\Gamma)$ and $|Q| < 1$, there exists a unique solution to the mixed variational problem (3). If $Q = 1$ a unique solution exists provided κ is not a Dirichlet eigenvalue for the domain.*

Remark 2. *The existence of a unique solution u to the Helmholtz problem with Robin-type boundary conditions is well established, see e.g.* [20]. *We provide an alternative proof that shows the well-posedness of the solution of the mixed problem directly.*

Proof. We prove uniqueness of the solution $(u, -\frac{1}{ik}\nabla u)$ by showing that the homogenous problem with right hand side $g = 0$ delivers only the trivial solution. Testing the first equation with $\xi = \operatorname{div} \boldsymbol{\tau}$ for some $\boldsymbol{\tau} \in H(\operatorname{div}; \Omega)$, we obtain

$$(u, \operatorname{div} \boldsymbol{\tau})_\Omega = -(\frac{1}{i\kappa} \operatorname{div} \boldsymbol{v}, \operatorname{div} \boldsymbol{\tau})_\Omega.$$

Inserting this into the second line of (3), we get

$$(\frac{1}{i\kappa} \operatorname{div} \boldsymbol{v}, \operatorname{div} \boldsymbol{\tau})_\Omega + (i\kappa \boldsymbol{v}, \boldsymbol{\tau})_\Omega - (\frac{q}{\eta}\boldsymbol{v}_n, \boldsymbol{\tau}_n)_{\partial\Omega} = 0. \tag{4}$$

Testing for $\boldsymbol{\tau} = \boldsymbol{v}$, and taking the real part, we immediately see that wherever $|Q| < 1$ we have $\boldsymbol{v}_n = 0$ on Γ. If $Q = 1$ we cannot conclude that $\boldsymbol{v}_n = 0$.

Now take $\boldsymbol{\tau} = \operatorname{curl}\phi$ for some smooth scalar field ϕ. This implies

$$(i\kappa\boldsymbol{v}, \operatorname{curl}\phi)_\Omega = 0,$$

and Stokes' theorem yields

$$(\operatorname{curl}\boldsymbol{v}, \phi)_\Omega + (\boldsymbol{v}\times n, \phi)_{\partial\Omega} = 0.$$

From this we obtain $\operatorname{curl}\boldsymbol{v} = 0$ and $\boldsymbol{v}\times n = 0$, which means that $\boldsymbol{v}$ is a gradient of a function with vanishing trace. Thus we may write

$$\boldsymbol{v} = \frac{1}{i\kappa}\nabla w.$$

For this w, equation (4) implies

$$\begin{aligned} 0 &= (\operatorname{div}\nabla w, \operatorname{div}\boldsymbol{\tau})_\Omega - \kappa^2(\nabla w, \boldsymbol{\tau})_\Omega \\ &= (\operatorname{div}\nabla w + \kappa^2 w, \operatorname{div}\boldsymbol{\tau})_\Omega. \end{aligned}$$

Suppose $|Q| < 1$, then because $\operatorname{div} : H(\operatorname{div};\Omega) \to L^2(\Omega)$ is surjective [15], we obtain that w is a solution to the Helmholtz problem with vanishing Dirichlet and Neumann traces $w = \frac{1}{i\kappa}\frac{\partial w}{\partial n} = 0$. This implies $w = 0$ and thereby uniqueness. If $Q = 1$ we know that w satisfies the Helmholtz equation with vanishing Dirichlet data. Thus provided κ is not an eigenvalue, we again verify uniqueness.

We now prove existence. Selecting $\xi = \operatorname{div}\boldsymbol{\tau}$ in the first equation of (3) and using the resulting identity in the second equation shows that $\boldsymbol{v} \in V$ satisfies

$$(5)\quad (\operatorname{div}\boldsymbol{v}, \operatorname{div}\boldsymbol{\tau})_\Omega - \kappa^2(\boldsymbol{v}, \boldsymbol{\tau})_\Omega - i\kappa(\frac{q}{\eta}\boldsymbol{v}_n, \boldsymbol{\tau}_n)_{\partial\Omega} = (\frac{i\kappa}{\eta(1+Q)}g, \boldsymbol{\tau}_n)_{\partial\Omega} \qquad \forall\boldsymbol{\tau} \in V.$$

For the rest of the proof we shall assume for concreteness that $d = 3$. Then choosing $\boldsymbol{\tau} = \operatorname{curl}\boldsymbol{q}$ for some $\boldsymbol{q} \in H_0(\operatorname{div};\Omega)\cap H(\operatorname{curl};\Omega)$ shows that $(\boldsymbol{v}, \operatorname{curl}\boldsymbol{q}) = 0$, so that $\operatorname{curl}\boldsymbol{v} = 0$ as we might expect. Thus we define

$$V^{(0)} = H(\operatorname{div};\Omega)\cap H(\operatorname{curl}_0;\Omega)$$

where $H(\operatorname{curl}_0;\Omega) = \{\boldsymbol{v} \in H(\operatorname{curl};\Omega) \mid \operatorname{curl}\boldsymbol{v} = 0\}$. Then we can pose (5) with $V^{(0)}$ in place of V. The advantage is now that by Theorem 3.47 of [21], the imbedding of $V^{(0)}$ into $[L^2(\Omega)]^3$ is compact. Hence problem (5) with $V^{(0)}$ in place of V gives rise to an operator equation involving a compact perturbation of the identity. In this case, the Fredholm alternative shows that the previously proved uniqueness implies the existence of a solution to (5) and hence to the full mixed system. □

To discretize the problem, we need to define suitable discrete spaces $V_h \subset V$, $U_h \subset U$. In this paper these are constructed using standard Raviart-Thomas finite elements. Therefore, we use a conforming and regular finite element mesh $\mathcal{T}_h = \{T_j : j \in J_h\}$ consisting of tetrahedra in case of $\Omega \subset \mathbb{R}^3$ or triangles for $\Omega \subset \mathbb{R}^2$, such that $\overline{\Omega} = \bigcup_{j\in J_h}\overline{T}_j$. Here the mesh size h is the maximum diameter of all mesh elements. Let $\mathcal{F}_h = \{F_{ij} = \partial T_i \cap \partial T_j\} \cup \{F_j = \partial T_j \cap \Gamma\}$ denote the set of element interfaces or facets. Then $\mathcal{F}_h$ corresponds to the set of edges in two

dimensions or faces in three dimensions. Let n_j denote the unit outward normal of an element T_j.

We need to assume that the mesh is chosen so that Q is constant on each boundary face of the mesh (it can vary from face to face).

On an element T_j we define

$$U_{j,h} = P^p(T_j) \tag{6}$$

to consist of piecewise polynomial functions of maximum degree p. Then the global finite element space $U_h \subset U$ is given by

$$U_h = \left\{ u_h \in L^2(\Omega) \mid u_h|_{T_j} \in U_{h,j} \text{ for } j \in J_h \right\}$$

so that no inter-element continuity is assumed. For the vector variables we define the local space

$$V_{h,j} = RT_p(T_j) \tag{7}$$

where the Raviart-Thomas space RT_p, was introduced in [24, 22]. It consists of piecewise polynomial, vector-valued finite elements of degree $p+1$, for which the normal component is of degree p on each face (or along each edge in two dimensions). Then the global space $V_h \subset V$ is defined by

$$V_h = \left\{ \boldsymbol{v}_h \in H(\mathrm{div};\Omega) \mid \boldsymbol{v}_h|_{T_j} \in V_{h,j} \text{ for } j \in J_h \right\}.$$

Note that functions in the global Raviart-Thomas space V_h, have normal components that are continuous across element interfaces. The degrees of freedom of a function $\boldsymbol{v}_h \in V_h$ are of two types. For example, in three dimensions, one type is associated with faces F of a tetrahedron T:

$$\int_F \boldsymbol{v}_n p \, ds, \qquad \forall p \in P^p(F) \text{ and for all faces } F \text{ of } T,$$

and other type is associated with the interior of T:

$$\int_T \boldsymbol{v} \cdot \boldsymbol{q} \, dx \qquad \forall \boldsymbol{q} \in [P^{p-1}(T)]^3.$$

Similarly, in two dimensions, degrees of freedom can be associated with edges or triangles. We shall use the fact that basis functions associated with the interior of the element (for $p \geq 1$) have vanishing normal component on all faces. Similarly basis functions associated with a given face (or edge in two dimensions) have vanishing normal component on all other faces (resp. edges).

The next theorem shows that for h small enough, we have existence and uniqueness of a solution to the discrete problem (8 - 9).

Lemma 3. *Suppose either $|Q| < 1$ or $Q = 1$ and κ is not a Dirichlet eigenvalue for the domain. Then provided that the mesh size h is small enough, the discrete*

Raviart-Thomas problem of finding $(u_h, \boldsymbol{v}_h) \in U_h \times V_h$ *such that*

$$(i\kappa u_h, \xi_h)_\Omega + (\operatorname{div} \boldsymbol{v}_h, \xi_h)_\Omega = 0 \tag{8}$$

$$-(u_h, \operatorname{div} \boldsymbol{\tau}_h)_\Omega + (i\kappa \boldsymbol{v}_h, \boldsymbol{\tau}_h)_\Omega - (\frac{q}{\eta}\boldsymbol{v}_{h,n}, \boldsymbol{\tau}_{h,n})_{\partial\Omega} = (\frac{1}{\eta(1+Q)}g, \boldsymbol{\tau}_{h,n})_{\partial\Omega} \tag{9}$$

for all $(\xi_h, \boldsymbol{\tau}_h) \in U_h \times V_h$ *has a unique solution. Moreover, for* $h \to 0$ *the finite element solution converges to the solution of the Helmholtz equation.*

Proof. For a Dirichlet boundary condition, this theorem follows from the uniform spectral convergence results for Raviart-Thomas elements in [4]. Their analysis does not handle the case when $|Q| < 1$ because of the impedance boundary condition. To prove this case we first notice that the Raviart-Thomas spaces are a stable pair of spaces for the problem when $\kappa = i$ since the appropriate inf-sup and coercivity results are known (see for example [5]). By verifying discrete compactness for these spaces and boundary conditions along the lines of the proof of similar results for edge elements (see [21]) we can then apply the theory of collectively compact operators to derive the result. □

2.2. **The Ultra-Weak Variational Formulation.** We now recall a second, rather different, variational method called the UWVF of the Helmholtz equation [7]. In this method we consider a piecewise defined function u_j on T_j, $j \in J_h$ which satisfies the Helmholtz equation locally on each element

$$\Delta u_j + \kappa^2 u_j = 0 \text{ in } T_j.$$

Then, to have a solution of the global problem, we need to enforce continuity of u and $\frac{1}{i\kappa}\frac{\partial u}{\partial n}$ across element interfaces. Using impedance traces, we require on each face F_{ij} (or edge) between elements T_i and T_j:

$$\left(\frac{1}{i\kappa}\frac{\partial u_i}{\partial n_i} + \eta u_i\right)\Big|_{\partial T_i} = \left(-\frac{1}{i\kappa}\frac{\partial u_j}{\partial n_j} + \eta u_j\right)\Big|_{\partial T_j}, \tag{10}$$

$$\left(\frac{1}{i\kappa}\frac{\partial u_i}{\partial n_i} - \eta u_i\right)\Big|_{\partial T_i} = \left(-\frac{1}{i\kappa}\frac{\partial u_j}{\partial n_j} - \eta u_j\right)\Big|_{\partial T_j}. \tag{11}$$

Here we have extended η from $L^\infty(\Gamma)$ to $L^\infty(\mathcal{F}_h)$ by unity (or in fact by a positive bounded function). The boundary condition on $F_j \subset \Gamma$ reads

$$\frac{1}{i\kappa}\frac{\partial u_j}{\partial n} - \eta u_j = Q\left[\frac{1}{i\kappa}\frac{\partial u_j}{\partial n} + \eta u_j\right] + g \quad \text{on } F_j.$$

We introduce the space X of impedance traces on element interfaces

$$X := \Pi_{j\in J_h} X_j, \quad X_j := L^2(\partial T_j).$$

For a general vector function $\mathcal{X} \in X$, the jth component, where $j \in J_h$, of $\mathcal{X}$ is denoted by $\mathcal{X}_j \in X_j$. We define the inner product on X

$$\begin{aligned}\langle \mathcal{X}, \mathcal{Y} \rangle_X &:= \sum_{j \in J_h} \langle \mathcal{X}_j, \mathcal{Y}_j \rangle_{X_j}, \\ \langle \mathcal{X}_j, \mathcal{Y}_j \rangle_{X_j} &:= \int_{\partial T_j} \frac{1}{\eta} \mathcal{X}_j \overline{\mathcal{Y}_j}\, ds.\end{aligned}$$

When performing integration only on the boundary Γ, we write $\langle \cdot, \cdot \rangle_{X,\Gamma}$ for

$$\langle \mathcal{X}, \mathcal{Y} \rangle_{X,\Gamma} := \sum_{j \in J_h} \int_{\partial T_j \cap \Gamma} \frac{1}{\eta} \mathcal{X}_j \overline{\mathcal{Y}_j}\, ds.$$

Note that any $\mathcal{X} \in X$ has two values $\mathcal{X}_i, \mathcal{X}_j$ on each facet $F_{ij} = \partial T_i \cap \partial T_j$, corresponding to the two adjacent elements, and one value $\mathcal{X}_j$ on each boundary facet $F_j \subset \Gamma$.

On this space, we define two operators. The first, $\Pi : X \to X$, interchanges the two values of $\mathcal{X}$ on internal facets F_{ij}. On boundary facets F_j, it helps to take care of the boundary condition:

$$\begin{aligned}(\Pi_j \mathcal{X})|_{F_{ij}} &= \mathcal{X}_i|_{F_{ij}} \qquad \text{for } F_{ij} \in \mathcal{F}_h \text{ internal}, \\ (\Pi_j \mathcal{X})|_{F_j} &= -Q\mathcal{X}_j|_{F_j} \quad \text{for } F_j \in \mathcal{F}_h, F_j \subset \Gamma.\end{aligned}$$

The second operator, $F : X \to X$, maps incoming to outgoing impedance traces. It is defined element by element. For $T_j \in \mathcal{T}_h$, the jth component $F_j \mathcal{X}_j$ depends only on $\mathcal{X}_j$. We can compute it using an auxiliary function $w_j \in H^1(T_j)$, that satisfies the adjoint Helmholtz equation, for which the incoming impedance trace is given by $\mathcal{X}_j$:

$$\begin{aligned}\Delta w_j + \kappa^2 w_j &= 0 \qquad \text{in } T_j, \\ \frac{1}{i\kappa} \frac{\partial w_j}{\partial n_j} + \eta w_j &= \mathcal{X}_j \quad \text{on } \partial T_j.\end{aligned} \tag{12}$$

Then we define $F_j \mathcal{X}_j$ to be the outgoing trace

$$F_j \mathcal{X}_j := -\frac{1}{i\kappa} \frac{\partial w_j}{\partial n_j} + \eta w_j \quad \text{on } \partial T_j.$$

To rewrite the continuity conditions on the impedance fluxes (10), (11), let $\mathcal{X} \in X$ be the function consisting of impedance traces of the solution u,

$$\mathcal{X}_j = \left(\frac{1}{i\kappa} \frac{\partial u_j}{\partial n_j} + \eta u_j \right) \Big|_{\partial T_j}.$$

Then we have for an element T_j

$$F_j \mathcal{X}_j = \left(-\frac{1}{i\kappa} \frac{\partial u_j}{\partial n_j} + \eta u_j \right) \Big|_{\partial T_j}.$$

On internal facets F_{ij} and boundary facets F_j, Π evaluates to

$$(\Pi_j \mathcal{X})|_{F_{ij}} = \left(\frac{1}{i\kappa} \frac{\partial u_i}{\partial n_i} + \eta u_i \right) \Big|_{F_{ij}}, \quad (\Pi_j \mathcal{X})|_{F_j} = -Q \left(\frac{1}{i\kappa} \frac{\partial u_j}{\partial n_j} + \eta u_j \right) \Big|_{F_j}.$$

Therefore we can rewrite the continuity conditions (10), (11) and the impedance boundary condition in a single equation

$$F\mathcal{X} - \Pi\mathcal{X} + \tilde{g} = 0,$$

where $\tilde{g} \in X$ is the extension by zero of g to the faces of the mesh away from the boundary.

The following fundamental properties of Π and F were shown in [6, 7].

Lemma 4. *(Cessenat and Després) Let $\Pi : X \to X$, $F : X \to X$ be defined as above. There holds*

- *If $|Q| \leq 1$, then $\|\Pi\|_{X \to X} \leq 1$.*
- *If $\kappa \in \mathbb{R}$, then F is an isometry, $F^*F = id$.*

Operating by F^*, we obtain the ultra-weak variational formulation (UWVF) of the Helmholtz equation

$$\mathcal{X} - F^*\Pi\mathcal{X} = -F^*\tilde{g}.$$

The corresponding Galerkin formulation is to seek $\mathcal{X} \in X$ such that

$$\langle \mathcal{X}, \mathcal{Y} \rangle_X - \langle \Pi\mathcal{X}, F\mathcal{Y} \rangle_X = -\langle \tilde{g}, F\mathcal{Y} \rangle_X \quad \forall \mathcal{Y} \in X.$$

Cessenat and Després [7] show that this problem has a unique solution for $|Q| < 1$.

3. Hybridization techniques

In this section, we present two ways of hybridizing the Raviart-Thomas method. First, we consider a method based on a finite element implementation of the UWVF, where the unknowns correspond to in- and outgoing fluxes $\pm \boldsymbol{v}_n + \eta u$ [7]. Then we derive a method where we regain normal continuity of the flux field by means of Lagrange multipliers and use consistent penalty terms to improve stability. The new unknowns resemble the scalar field u and the normal flux $\boldsymbol{v}_n$ on element interfaces. We observe that the two formulations are equivalent to the original Raviart-Thomas method, and that the UWVF is a special case of the Lagrange multiplier based method.

3.1. The discrete finite element UWVF.

To discretize the UWVF Cessenat and Després use plane waves on each element, and we shall describe this method briefly in Section 4.3. In this section we investigate instead a new method based on mixed finite elements. We first construct a finite element subspace $X_h \subset X$. We choose $X_h = \Pi_{j \in J_h} X_{h,j}$, where $X_{h,j}$ is the space of piecewise polynomials of degree p on the facets of element T_j:

$$X_{h,j} = \{ \xi_h \in L^2(\partial T_j) \mid \xi_h|_F \in P^p(F), \text{ for each face (edge) } F \text{ of } T_j \}.$$

Note that equivalently

$$X_{h,j} = \{\xi_h \in L^2(\partial T_j) \mid \xi_h = \boldsymbol{v}_{h,n} \text{ for some } \boldsymbol{v}_h \in RT_p(T_j)\}.$$

Next we replace F by a finite element approximation F_h using mixed finite elements. The computation of F_h can be done locally on each element, and the jth component of $F_h\mathcal{Y}_h$ depends only on $\mathcal{Y}_{h,j}$.

We define the discrete operator $F_h : X \to X$ component-wise using the local spaces defined in Section 2.1. For $\mathcal{Y}_j \in X_j$, let $(u_{h,j}, \boldsymbol{v}_{h,j}) \in U_{h,j} \times V_{h,j}$ be such that for all $\xi_{h,j} \in U_{h,j}, \boldsymbol{\tau}_{h,j} \in V_{h,j}$

$$\begin{aligned} (i\kappa u_{h,j}, \xi_{h,j})_{T_j} + (\operatorname{div} \boldsymbol{v}_{h,j}, \xi_{h,j})_{T_j} &= 0, \\ (u_{h,j}, \operatorname{div} \boldsymbol{\tau}_{h,j})_{T_j} - (i\kappa \boldsymbol{v}_{h,j}, \boldsymbol{\tau}_{h,j})_{T_j} & \end{aligned} \tag{13}$$

$$-(\frac{1}{\eta}\boldsymbol{v}_{h,j,n_j}, \boldsymbol{\tau}_{h,j,n_j})_{\partial T_j} = (\frac{1}{\eta}\mathcal{Y}_j, \boldsymbol{\tau}_{h,j,n_j})_{\partial T_j}. \tag{14}$$

Then we define

$$F_{h,j}\mathcal{Y}_j = \mathcal{Y}_j + 2\boldsymbol{v}_{h,j,n_j}.$$

Note that, since normal traces of RT_p functions are in the space P^p on each face used to construct $X_{h,j}$ we have $F_h : X_h \to X_h$. This holds even if p varies from element to element.

The finite element discrete UWVF is now to find a Galerkin approximation $\mathcal{X}_h \in X_h$ such that

$$\langle \mathcal{X}_h, \mathcal{Y}_h\rangle_X - \langle \Pi\mathcal{X}_h, F_h\mathcal{Y}_h\rangle_X = -\langle \tilde{g}, F_h\mathcal{Y}_h\rangle_X \quad \forall \mathcal{Y}_h \in X_h. \tag{15}$$

For the analysis of the discrete UWVF, we introduce an operator $A_{h,j} : U_{h,j} \times V_{h,j} \to U_{h,j} \times V_{h,j}$, which corresponds to the left hand side of (13)-(14), and $B_j : U_{h,j} \times V_{h,j} \to X_{h,j}$, which is related to its right hand side via

$$\begin{aligned} \langle A_{h,j}(u_h, \boldsymbol{v}_h); \xi_h, \boldsymbol{\tau}_h\rangle_{U_j \times V_j} &:= (i\kappa u_h + \operatorname{div} \boldsymbol{v}_h, \xi_h)_{T_j} + (u_h, \operatorname{div} \boldsymbol{\tau}_h)_{T_j} - (i\kappa \boldsymbol{v}_h, \boldsymbol{\tau}_h)_{T_j} \\ &\quad -(\frac{1}{\eta}\boldsymbol{v}_{h,n_j}, \boldsymbol{\tau}_{h,n_j})_{\partial T_j}, \qquad \forall \boldsymbol{\tau}_h \in V_{h,j}, \xi_h \in U_{h,j}, \\ \langle B_{h,j}(u_h, \boldsymbol{v}_h), \mathcal{Y}_h\rangle_{X_j} &:= (\frac{1}{\eta}\boldsymbol{v}_{h,n_j}, \mathcal{Y}_h)_{\partial T_j}, \qquad \forall \mathcal{Y}_h \in X_{h,j}. \end{aligned}$$

Then, for $\mathcal{Y}_j \in X_{h,j}$, we can rewrite the local system (13)-(14) as

$$\langle A_{h,j}(u_{h,j}, \boldsymbol{v}_{h,j}); \xi_{h,j}, \boldsymbol{\tau}_{h,j}\rangle_{U_j \times V_j} = \langle B^*_{h,j}(\mathcal{Y}_j); \xi_{h,j}, \boldsymbol{\tau}_{h,j}\rangle_{U_j \times V_j} \tag{16}$$

for all $\forall \xi_{j,h} \in U_{h,j}$ and $\boldsymbol{\tau}_{h,j} \in V_{h,j}$. Thereby $F_{h,j}$ can be written explicitly as

$$F_{h,j}\mathcal{Y}_{h,j} = (id + 2B_{h,j}A^{-1}_{h,j}B^*_{h,j})(\mathcal{Y}_{h,j}).$$

Lemma 5. *If h is small enough, the discrete operator $F_h : X_h \to X_h$ is well defined and is an isometry.*

Remark 6. *The space X can be written $X = X_h \oplus X_h^\perp$ where $X_h^\perp$ is the orthogonal complement of X_h using the inner product for X. For a function $\mathcal{Y} \in X_h^\perp$, we have $F_h(\mathcal{Y}) = \mathcal{Y}$. Thus F_h is an isometry on X also.*

Proof. The restriction on h is needed to ensure that the local mixed problem (13)-(14) has a solution. For $\mathcal{Y}_h \in X_h$, we evaluate $\|F_h\mathcal{Y}_h\|_X^2 = \sum_{j\in J_h} \|F_{h,j}\mathcal{Y}_{h,j}\|_{X_j}^2$. On an element $T_j \in \mathcal{T}_h$, let $(u_{h,j}, \boldsymbol{v}_{h,j}) = A_{h,j}^{-1}B_{h,j}^*\mathcal{Y}_{h,j}$ be the local solution of (13)-(14), then

$$\begin{aligned} \|F_{h,j}\mathcal{Y}_{h,j}\|_{X_j}^2 &= (\frac{1}{\eta}(\mathcal{Y}_{h,j} + 2\boldsymbol{v}_{h,j,n_j}), \mathcal{Y}_{h,j} + 2\boldsymbol{v}_{h,j,n_j})_{\partial T_j} \\ &= \int_{\partial T_j} \frac{1}{\eta}|\mathcal{Y}_{h,j}|^2 + \frac{4}{\eta}|\boldsymbol{v}_{h,j,n_j}|^2 + 4\frac{1}{\eta}Re\left(\mathcal{Y}_{h,j}\,\overline{\boldsymbol{v}}_{h,j,n_j}\right)\,dx. \end{aligned} \tag{17}$$

To evaluate the last term above, we investigate the local problem further. Setting $\boldsymbol{\tau}_{h,j} = \boldsymbol{v}_{h,j}$, and $\xi_{h,j} = -u_{h,j}$ in (13)-(14) and adding the resulting equalities, we obtain

$$\int_T u_{h,j}\overline{\operatorname{div}\boldsymbol{v}_{h,j}} - \overline{u_{h,j}}\operatorname{div}\boldsymbol{v}_{h,j} - i\kappa|u_{h,j}|^2 - i\kappa|\boldsymbol{v}_{h,j}|^2\,dx = \int_{\partial T_j}\frac{1}{\eta}(\mathcal{Y}_{h,j} + \boldsymbol{v}_{h,j,n_j})\overline{\boldsymbol{v}}_{h,j,n_j}\,ds.$$

As the left-hand side of this equation is purely imaginary, by taking the real part we get

$$\int_{\partial T_j}\frac{1}{\eta}Re(\mathcal{Y}_{h,j}\,\overline{\boldsymbol{v}_{h,j,n_j}})\,ds = -\int_{\partial T_j}\frac{1}{\eta}|\boldsymbol{v}_{,hj,n_j}|^2\,ds.$$

Inserting this into equation (17) shows

$$\|F_{h,j}\mathcal{Y}_{h,j}\|_{X_j}^2 = \|\mathcal{Y}_{h,j}\|_{X_j}^2.$$

Therefore F_h is an isometry on X_h. □

Theorem 7. *If the mesh size h is small enough and the polynomial degree p is the same on all elements, the discrete UWVF (15) has a unique solution. The local solution $(u_h, \boldsymbol{v}_h)$ computed from the impedance traces $\mathcal{X}_h$ coincides with the solution of the standard Raviart-Thomas system.*

Remark 8. *This theorem can be extended to the case of variable order elements provided a single polynomial degree is chosen for each face (or edge). We choose p_{ij} on F_{ij} and then if $\mathcal{X}_i \in X_{h,i}$ we have $\mathcal{X}_i|_{F_{ij}} \in P^{p_{ij}}(F_{ij})$ and if $\mathcal{X}_j \in X_{h,j}$ we also have $\mathcal{X}_j|_{F_{ij}} \in P^{p_{ij}}(F_{ij})$. In addition the finite element space $U_{h,i}$ and $V_{h,i}$ have to be chosen as a stable mixed pair of spaces such that if $\boldsymbol{\tau}_h \in V_{h,i}$ then $\boldsymbol{\tau}_{h,i,n_i}|_{F_{ij}} \in P^{p_{ij}}(F_{ij})$. The construction of such elements is possible in the framework of hp-mixed methods* [10]. *We shall not give details of the variable degree scheme here since it very much complicates notation.*

Proof. Due to the fact that F_h is an isometry, $F_h^*F_h = id$, we obtain directly from equation (15) that

$$\langle F_h\mathcal{X}_h, F_h\mathcal{Y}_h\rangle_X - \langle \Pi\mathcal{X}_h, F_h\mathcal{Y}_h\rangle_X = -\langle \tilde{g}, F_h(\mathcal{Y}_h)\rangle_X$$

But $F_h : X_h \to X_h$ (and is invertible) and $\Pi : X_h \to X_h$ since we have assumed that the polynomial degree is the same on all elements and Q is constant on each

face, so that we have

$$F_h \mathcal{X}_h - \Pi \mathcal{X}_h = -P_h \tilde{g}$$

where $P_h : X \to X_h$ is the orthogonal projection (weighted by $1/\eta$).

On an interior facet $F_{ij} = \partial T_i \cap \partial T_j$ this implies

$$F_{h,j} \mathcal{X}_{h,j} = \mathcal{X}_{h,i} \quad \text{and} \quad F_{h,i} \mathcal{X}_{h,i} = \mathcal{X}_{h,j}.$$

Let $(u_{h,i}, \boldsymbol{v}_{h,i}) \in U_{h,i} \times V_{h,i}$, and $(u_{h,j}, \boldsymbol{v}_{h,j}) \in U_{h,j} \times V_{h,j}$ denote the finite element solutions for the local problem (13)-(14) on T_i and T_j with boundary data $\mathcal{X}_{h,i}, \mathcal{X}_{h,j}$ respectively. Then the above equations can be rewritten as

$$\mathcal{X}_{h,j} + 2\boldsymbol{v}_{h,j,n_j} = \mathcal{X}_{h,i} \quad \text{and} \quad \mathcal{X}_{h,i} + 2\boldsymbol{v}_{h,i,n_i} = \mathcal{X}_{h,j},$$

which implies normal continuity of the composite function $\boldsymbol{v}_h$ defined by $\boldsymbol{v}_h|_{T_j} = \boldsymbol{v}_{h,j}$ for each j. Therefore, $\boldsymbol{v}_h$ lies in the global Raviart-Thomas space V_h. It remains to show, that the composite functions $(u_h, \boldsymbol{v}_h) \in U_h \times V_h$ satisfy the discrete mixed system (8)-(9).

One immediately sees that the first equation in the mixed formulation (8) is equivalent to equation (13). Now let $\boldsymbol{\tau}_{h,ij}$ be a standard basis function of V_h associated with an internal facet F_{ij} so that its normal trace vanishes on all facets $F \neq F_{ij}$. Then equation (14) evaluated on T_i and T_j gives

$$\begin{array}{rcl} (u_{h,i}, \operatorname{div} \boldsymbol{\tau}_{h,ij})_{T_i} - (i\kappa \boldsymbol{v}_{h,i}, \boldsymbol{\tau}_{h,ij})_{T_i} & = & (\frac{1}{\eta}(\mathcal{X}_{h,i} + \boldsymbol{v}_{h,i,n_i}), \boldsymbol{\tau}_{h,ij,n_i})_{F_{ij}}, \\ (u_{h,j}, \operatorname{div} \boldsymbol{\tau}_{h,ij})_{T_j} - (i\kappa \boldsymbol{v}_{h,j}, \boldsymbol{\tau}_{h,ij})_{T_j} & = & (\frac{1}{\eta}(\mathcal{X}_{h,j} + \boldsymbol{v}_{h,j,n_j}), \boldsymbol{\tau}_{h,ij,n_j})_{F_{ij}}. \end{array} \tag{18}$$

Adding these equations, and using the fact that the composite function $\boldsymbol{v}_h$ is normal continuous, we obtain

$$(u_h, \operatorname{div} \boldsymbol{\tau}_{h,ij})_{T_i \cup T_j} - (i\kappa \boldsymbol{v}_h, \boldsymbol{\tau}_{h,ij})_{T_i \cup T_j} = (\frac{1}{\eta}(\mathcal{X}_{h,i} - \mathcal{X}_{h,j} + 2\boldsymbol{v}_{h,n_i}), \boldsymbol{\tau}_{h,ij,n_i})_{F_{ij}} = 0.$$

Therefore the global Raviart-Thomas equation (9) is satisfied for $\boldsymbol{\tau}_h = \boldsymbol{\tau}_{h,ij}$. For internal basis functions (having vanishing normal traces on all faces), it is obvious that (9) is equivalent to equation (14).

On a boundary facet $F_j \subset \Gamma$, we have $\Pi_j \mathcal{X}_h = -Q\mathcal{X}_{h,j}$, and therefore $F_{h,j}\mathcal{X}_{h,j} = -Q\mathcal{X}_{h,j} - P_h\tilde{g}$, which implies

$$\mathcal{X}_{h,j} + 2\boldsymbol{v}_{h,j,n_j} = -Q\mathcal{X}_{h,j} - P_h\tilde{g} \qquad \text{on } \Gamma_j.$$

Let now $\boldsymbol{\tau}_{h,j}$ be a Raviart-Thomas basis function with non vanishing normal component on F_j (and zero on all others). Then equation (14) reads

$$\begin{array}{rcl} (u_{h,j}, \operatorname{div} \boldsymbol{\tau}_{h,j})_{T_j} - (i\kappa \boldsymbol{v}_{h,j}, \boldsymbol{\tau}_{h,j})_{T_j} & = & (\frac{1}{\eta}\left(\mathcal{X}_{h,j} + \boldsymbol{v}_{h,j,n_j}\right), \boldsymbol{\tau}_{h,j,n_j})_{F_j} \\ & = & (-\frac{q}{\eta}\boldsymbol{v}_{h,j,n_j} - \frac{1}{\eta}\frac{1}{1+Q}P_h\tilde{g}, \boldsymbol{\tau}_{h,j,n_j})_{F_j} \\ & = & (-\frac{q}{\eta}\boldsymbol{v}_{h,j,n_j} - \frac{1}{\eta}\frac{1}{1+Q}g, \boldsymbol{\tau}_{h,j,n_j})_{F_j} \end{array}$$

where the last equality holds because P_h is defined face by face due to the discontinuous basis functions in $X_{h,j}$. This means that the Raviart-Thomas system is satisfied for $\boldsymbol{\tau}_{h,j}$.

Since we have existence and uniqueness of the global discrete problem for sufficiently small mesh size h, we obtain unique local solutions $(u_{h,j}, \boldsymbol{v}_{h,j})$ by restriction to element T_j. Then $\mathcal{X}_{h,i}|_{F_{ij}}$ and $\mathcal{X}_{h,j}|_{F_{ij}}$ are determined uniquely by (18). □

3.2. **Facet-based hybridization.** In this subsection we derive another, more standard, discrete hybrid problem formulation. As for the discrete Raviart-Thomas problem, we use spaces of piecewise polynomial functions to approximate $(u, \boldsymbol{v})$. But, in contrast to the Raviart-Thomas case, we do not require continuity of the normal flux $\boldsymbol{v}_{h,n}$ across element interfaces. Using the local spaces $U_{h,j}, V_{h,j}$ (see (6) and (7)), define

$$U_h := \Pi_{j\in J_h} U_{h,j}, \quad \tilde{V}_h := \Pi_{j\in J_h} V_{h,j}.$$

To derive equations for the discrete variables, we multiply the mixed version of the Helmholtz equation (2) by test functions $(\boldsymbol{\tau}_h, \xi_h) \in \tilde{V}_h \times U_h$ and integrate by parts on each element. Then

$$\begin{aligned} -(i\kappa u, \xi_h)_\Omega - (\operatorname{div} \boldsymbol{v}, \xi_h)_\Omega &= 0, \\ -\sum_{j\in J_h} (u, \operatorname{div} \boldsymbol{\tau}_{h,j})_{T_j} + (i\kappa \boldsymbol{v}, \boldsymbol{\tau}_h)_\Omega + \sum_{j\in J_h} (u, \boldsymbol{\tau}_{h,j,n_j})_{\partial T_j} &= 0. \end{aligned}$$

The discrete problem is now obtained by replacing u and $\boldsymbol{v}$ above with $u_h \in U_h$ and $\boldsymbol{v}_h \in \tilde{V}_h$. In addition, we enforce continuity of $\boldsymbol{v}_{h,n}$ by means of a Lagrangian multiplier. Therefore, we introduce a discretization of the trace of the scalar field $u|_F$ for each face in the mesh denoted u_h^F. This is defined on the set of element facets $\mathcal{F}_h$. In particular we define the space

$$U_h^F := \{\xi_h^F \in L^2(\mathcal{F}) : \xi_h^F|_{F_{ij}} \in P^p(F_{ij})\}.$$

Then $(u_h, \boldsymbol{v}_h, u_h^F) \in U_h \times \tilde{V}_h \times U_h^F$ satisfy

$$\begin{aligned} -(i\kappa u_h, \xi_h)_\Omega - (\operatorname{div} \boldsymbol{v}_h, \xi_h)_\Omega &= 0, \\ -\sum_{j\in J_h} (u_h, \operatorname{div} \boldsymbol{\tau}_{h,j})_{T_j} + (i\kappa \boldsymbol{v}_h, \boldsymbol{\tau}_h)_\Omega + \sum_{j\in J_h} (u_h^F, \boldsymbol{\tau}_{h,j,n_j})_{\partial T_j} &= 0, \end{aligned}$$

for all $(\xi_h, \boldsymbol{\tau}_h) \in U_h \times \tilde{V}_h$.

The normal continuity of the flux across an internal facet F_{ij} can now be imposed by

$$(\boldsymbol{v}_{h,j,n_j} + \boldsymbol{v}_{h,i,n_i}, \xi_h^F)_{F_{ij}} = 0 \quad \forall \xi^F \in U^F.$$

On the outer boundary, we have, due to the generalized impedance boundary condition,

$$(\boldsymbol{v}_{h,n} + \eta u_h^F, \xi_h^F)_\Gamma = (-Q\left[-v_{h,n} + \eta u_h^F\right] - g, \xi_h^F)_\Gamma \quad \forall \xi_h^F \in U^F.$$

Reordering these terms element by element, we obtain

$$\sum_{j\in J_h}(\boldsymbol{v}_{h,j,n_j},\xi_h^F)_{\partial T_j}+(\frac{\eta}{q}u_h^F,\xi_h^F)_\Gamma=-(\frac{1}{1-Q}g,\xi_h^F)_\Gamma\quad\forall\xi_h^F\in U^F.$$

In summary, we obtain a system, equivalent to the Raviart-Thomas system, of finding $(u_h,\boldsymbol{v}_h,u_h^F)\in U_h\times\tilde{V}_h\times U_h^F$ such that

$$\begin{aligned}
-(i\kappa u_h,\xi_h)_\Omega-(\operatorname{div}\boldsymbol{v}_h,\xi_h)_\Omega &= 0 \qquad \forall\xi_h\in U_h\\
-\sum_{j\in J_h}(u_{h,j},\operatorname{div}\boldsymbol{\tau}_{h,j})_{T_j}+(i\kappa\boldsymbol{v}_h,\boldsymbol{\tau}_h)_\Omega+\sum_{j\in J_h}(u_h^F,\boldsymbol{\tau}_{h,j,n_j})_{\partial T_j} &= 0 \qquad \forall\boldsymbol{\tau}_h\in\tilde{V}_h\\
\sum_{j\in J_h}(\boldsymbol{v}_{h,j,n_j},\xi_h^F)_{\partial T_j}+(\tfrac{\eta}{q}u_h^F,\xi_h^F)_\Gamma &= -(\tfrac{1}{1-Q}g,\xi_h^F)_\Gamma\\
&\qquad\forall\xi_h^F\in U_h^F.
\end{aligned}$$

Numerical tests of this scheme (not shown) show poor convergence of the iterative schemes we tried (preconditioned Conjugate Gradients). Therefore to stabilize the method we then introduce a second scalar-valued unknown $\boldsymbol{v}_h^F$ on the set of facets, which corresponds to the normal flux. Because the outward unit normal changes its sign when switching from element T_i to a neighboring element T_j, also the normal flux $\boldsymbol{v}_{h,n}$ flips sign. We put an index n to indicate this direction also for the trace field $\boldsymbol{v}_h^F$. This means, on facet F_{ij}, we have $\boldsymbol{v}_{h,n_i}^F=-\boldsymbol{v}_{h,n_j}^F$. Let V_h^F be the space of all such functions, which are piecewise P^p

$$V_h^F:=\{\boldsymbol{\tau}_h^F\in L^2(\mathcal{F}):\boldsymbol{\tau}_{h,n_i}^F=-\boldsymbol{\tau}_{h,n_j}^F\in P^p(F_{ij})\}.$$

For later analysis, note that both U_h^F and V_h^F are subspaces of X_h used in the discrete UWVF. Moreover, each $\mathcal{X}\in X_h$ can be written as a composition $\mathcal{X}_h=\eta u_h^F+\boldsymbol{v}_{h,n}^F$, where u_h^F is the average of the two-valued function $\mathcal{X}_h$, and $\boldsymbol{v}_{h,n}^F$ corresponds to the jump, provided η is constant on each face (or edge).

Since the normal traces of RT_p finite element functions in V_h span this space, we can add a consistent stabilization term

$$-\sum_{j\in J_h}(\boldsymbol{v}_{h,j,n_j}-\boldsymbol{v}_{h,n_j}^F,\boldsymbol{\tau}_{h,j,n_j}-\boldsymbol{\tau}_{h,n_j}^F)_{\partial T_j},$$

and obtain an equivalent equation.

An abstract formulation of this problem is to find $(u_h,\boldsymbol{v}_h,u_h^F,\boldsymbol{v}_h^F)\in U_h\times\tilde{V}_h\times U_h^F\times V_h^F$ such that

$$\mathcal{B}_h(u_h,\boldsymbol{v}_h,u_h^F,\boldsymbol{v}_h^F;\xi_h,\boldsymbol{\tau}_h,\xi_h^F,\boldsymbol{\tau}_h^F)=-(\frac{1}{1-Q}g,\xi_h^F)_\Gamma$$

for all $(\xi_h, \boldsymbol{\tau}_h, \xi_h^F, \boldsymbol{\tau}_h^F) \in U_h \times \tilde{V}_h \times U_h^F \times V_h^F$ where

$$\begin{aligned}\mathcal{B}_h(u_h, \boldsymbol{v}_h, u_h^F, \boldsymbol{v}_h^F; \xi_h, \boldsymbol{\tau}_h, \xi_h^F, \boldsymbol{\tau}_h^F) = \sum_{j\in J_h} \Big\{ &- (i\kappa u_{h,j} + \operatorname{div} \boldsymbol{v}_{h,j}, \xi_{h,j})_{T_j} - \\ &(u_{h,j}, \operatorname{div} \boldsymbol{\tau}_{h,j})_{T_j} + (i\kappa \boldsymbol{v}_{h,j}, \boldsymbol{\tau}_{h,j})_{T_j} + (u_h^F, \boldsymbol{\tau}_{h,j,n_j})_{\partial T_j} + \\ &(\boldsymbol{v}_{h,j,n_j}, \xi_h^F)_{\partial T_j} - (\frac{1}{\eta}(\boldsymbol{v}_{h,j,n_j} - \boldsymbol{v}_{h,n_j}^F), \boldsymbol{\tau}_{h,j,n_j} - \boldsymbol{\tau}_{h,n_j}^F)_{\partial T_j} \Big\} + (\frac{\eta}{q} u_h^F, \xi_h^F)_\Gamma.\end{aligned}$$

Using the operators $A_{h,j}, B_{h,j}$ defined in the previous subsection, we see

$$\begin{aligned}\mathcal{B}_h(u_h, \boldsymbol{v}_h, u_h^F \boldsymbol{v}_h^F\ \ \xi_h, \boldsymbol{\tau}_h, \xi_h^F \boldsymbol{\tau}_h^F) = \sum_{j\in J_h} \Big\{ &\langle A_{h,j}^*(-u_{h,j}, \boldsymbol{v}_{h,j}); -\xi_{h,j}, \boldsymbol{\tau}_{h,j}\rangle_{U_j \times V_j} + \\ &\langle \boldsymbol{v}_h^F + \eta u_h^F, B_{h,j}\boldsymbol{\tau}_{h,j}\rangle_{X_j} + \langle B_{h,j}\boldsymbol{v}_{h,j}, \eta\xi_h^F\rangle_{X_j} + \langle B_{h,j}(\boldsymbol{v}_{h,j} - \boldsymbol{v}_h^F), \boldsymbol{\tau}_h^F\rangle_{X_j} \Big\} + \\ &\langle \frac{\eta}{q} u_h^F, \eta\xi_h^F\rangle_{X,\Gamma}.\end{aligned}$$

In this formulation, the degrees of freedom for u_h and $\boldsymbol{v}_h$ are associated element by element. This means that they can be eliminated locally. On element T_j, we solve the sub-system

$$\langle A_{h,j}^*(-u_{h,j}, \boldsymbol{v}_{h,j}); -\xi_h, \boldsymbol{\tau}_{h,j}\rangle_{U_j \times V_j} = -\langle B_{h,j}^*(\boldsymbol{v}_h^F + \eta u_h^F), \boldsymbol{\tau}_{h,j}\rangle_{V_j},$$

which yields the solution

$$(-u_{h,j}, \boldsymbol{v}_{h,j}) = -(A_{h,j}^*)^{-1} B_{h,j}^*(\boldsymbol{v}_h^F + \eta u_h^F).$$

Hence, the global problem reduces to the Schur complement system

$$\langle \mathcal{S}_h(u_h^F, \boldsymbol{v}_h^F); \xi_h^F, \boldsymbol{\tau}_h^F\rangle_X = -\langle \frac{1}{1-Q} g, \eta\xi_h^F\rangle_{X,\Gamma}, \tag{19}$$

where the Schur operator $\mathcal{S}_h$ is defined by the relation

$$\begin{aligned}\langle \mathcal{S}_h(u_h^F, \boldsymbol{v}_h^F); \xi_h^F, \boldsymbol{\tau}_h^F\rangle_X \ \ = \ \ - \sum_{j\in J_h} \Big\{ &\langle B_{h,j}(A_{h,j}^*)^{-1} B_{h,j}^*(\boldsymbol{v}_h^F + \eta u_h^F), \boldsymbol{\tau}_h^F + \eta\xi_h^F\rangle_{X_j} + \\ &\langle \boldsymbol{v}_h^F, \boldsymbol{\tau}_h^F\rangle_{X_j} \Big\} + \langle \eta u_h^F, \frac{\eta}{q}\xi_h^F\rangle_{X,\Gamma}.\end{aligned}$$

Lemma 9. *Provided h is sufficiently small, the hybridized discrete Helmholtz problem (19) has a unique solution. The flux approximation lies in the global Raviart-Thomas space, $\boldsymbol{v}_h \in V_h$. The formulation is equivalent to the Raviart-Thomas method.*

Proof. As we have seen when deriving the above system, it is equivalent to the Raviart-Thomas case. The flux function $\boldsymbol{v}_h$ has a continuous normal component across element interfaces, therefore it lies in the global Raviart-Thomas space. □

3.3. **Comparison of the hybridization strategies.** In this subsection, we compare the two methods we considered so far in this section. We will see that they are closely related by a change of variables, if η is piecewise constant on Γ. Already in [16], the UWVF was analyzed in a DG framework. We see a similar relation for the polynomial-based versions proposed above.

Throughout the following, let η be piecewise constant, and constant on each facet in the mesh. The function $\mathcal{X}_h \in X_h$ will denote a solution to the discrete ultra-weak variational formulation, we shall then construct a pair $(u_h^F, \boldsymbol{v}_h^F)$ and show that the pair is a solution to the corresponding hybridized finite element problem. We first investigate the relationship of these solutions on an interior facet.

Let $F_{ij} = \partial T_i \cap \partial T_j$ be an internal facet. Consider a solution $\mathcal{X}_h$ to the UWVF problem. Obviously, there exist unique $(u_h^F, \boldsymbol{v}_h^F) \in U_h^F \times V_h^F$ such that

$$\mathcal{X}_{h,j} = -\boldsymbol{v}_{h,n_j}^F + \eta u_h^F,\ \mathcal{X}_{h,i} = -\boldsymbol{v}_{h,n_i}^F + \eta u^F \quad \text{on } F_{ij}. \tag{20}$$

We show that these $(u_h^F, \boldsymbol{v}_h^F)$ satisfy the corresponding hybridized equation. As F_{ij} is a facet in the interior, if we use functions $\mathcal{Y}_h \in X_h$ that vanish on faces away from T_i and T_j the ultra-weak equation reads

$$\langle \mathcal{X}_h, \mathcal{Y}_h \rangle_X - \langle \Pi \mathcal{X}_h, F_h(\mathcal{Y}_h) \rangle_X = 0.$$

Recalling that $\mathcal{X}_{h,j} = -\boldsymbol{v}_{h,n_j}^F + \eta u_h^F$, we see that $\Pi \mathcal{X}_{h,j} = \mathcal{X}_{h,i} = \boldsymbol{v}_{h,n_j}^F + \eta u_h^F$. Testing with $\mathcal{Y}_{h,i} = \mathcal{Y}_{h,j} = \eta \xi_h^F$, which is continuous across F_{ij}, we obtain

$$\begin{aligned} 0 &= \sum_{k=i,j} \langle -\boldsymbol{v}_{h,n_k}^F + \eta u_h^F, \eta \xi_h^F \rangle_X - \langle \boldsymbol{v}_{h,n_k}^F + \eta u_h^F, (id + 2B_{h,k} A_{h,k}^{-1} B_{h,k}^*)(\eta \xi_h^F) \rangle_X \\ &= \sum_{k=i,j} -\langle 2\boldsymbol{v}_{h,n_k}^F, \eta \xi_h^F \rangle_X - \langle 2B_{h,k} (A_{h,k}^{-1})^* B_{h,k}^* (\boldsymbol{v}_{h,n_k}^F + \eta u_h^F), \eta \xi_h^F \rangle_X. \end{aligned}$$

As $\boldsymbol{v}_{h,n_k}^F$ flips sign when switching between T_i, T_j, the first term cancels out, and we obtain

$$0 = \sum_{k=i,j} \langle B_{h,k} (A_{h,k}^{-1})^* B_{h,k}^* (\boldsymbol{v}_{h,n_k}^F + \eta u_h^F), \eta \xi_h^F \rangle_X. \tag{21}$$

Now, we test for the jumping function $\mathcal{Y}_{h,i} = \boldsymbol{\tau}_{h,n_i}^F, \mathcal{Y}_{h,j} = \boldsymbol{\tau}_{h,n_j}^F = -\mathcal{Y}_{h,i}$.

$$\begin{aligned} 0 &= \sum_{k=i,j} \langle -\boldsymbol{v}_{h,n_k}^F + \eta u_h^F, \boldsymbol{\tau}_{h,n_k}^F \rangle_X - \langle \boldsymbol{v}_{h,n_k}^F + \eta u_h^F, (id + 2B_{h,k} A_{h,k}^{-1} B_{h,k}^*) \boldsymbol{\tau}_{h,n_k}^F \rangle_X \\ (22) &= \sum_{k=i,j} -\langle 2\boldsymbol{v}_{h,n_k}^F, \boldsymbol{\tau}_{h,n_k}^F \rangle_X - \langle 2B_{h,k} (A_{h,k}^{-1})^* B_{h,k}^* (\boldsymbol{v}_{h,n_k}^F + \eta u_h^F), \boldsymbol{\tau}_{h,n_k}^F \rangle_X. \end{aligned}$$

Adding the two equations (21), (22), we get an equivalent equation to the hybridized Helmholtz system (19).

Now, we consider a facet F_j lying on the boundary Γ. Let again $\mathcal{X}_h$ be a solution to the UWVF problem. Then we can find unique $(u_h^F, \boldsymbol{v}_h^F)$ such that

$$\mathcal{X}_{h,j} = -\boldsymbol{v}_{h,n_j}^F + \eta u_h^F, \quad \boldsymbol{v}_{h,n_j}^F + \eta u_h^F = -Q(-\boldsymbol{v}_{h,n_j}^F + \eta u_h^F) - P_h\tilde{g}. \tag{23}$$

This implies $\Pi\mathcal{X}_h = -Q(-\boldsymbol{v}_{h,n_j}^F + \eta u_h^F) = \boldsymbol{v}_{h,n_j}^F + u_h^F + P_h\tilde{g}$. For the test function $\mathcal{Y}_h$, we use

$$\mathcal{Y}_h = \boldsymbol{\tau}_{h,n_j}^F + \eta\xi_h^F, \qquad -\boldsymbol{\tau}_{h,n_j}^F + \eta\xi_h^F = 0.$$

With these choices the ultra-weak equation (15) transforms to

$$\langle -\boldsymbol{v}_{h,n_j}^F + \eta u_h^F, \boldsymbol{\tau}_{h,n_j}^F + \eta\xi_h^F\rangle_X - \langle \boldsymbol{v}_{h,n_j}^F + \eta u_h^F, (id + 2B_{h,j}A_{h,j}^{-1}B_{h,j}^*)(\boldsymbol{\tau}_{h,n_j}^F + \eta\xi_h^F)\rangle_X.$$

Using $\boldsymbol{v}_{h,n_j}^F = -\frac{1}{1-Q}P_h\tilde{g} - \frac{\eta}{q}u_h^F$ and $\boldsymbol{\tau}_{h,n_j}^F = \eta\xi_h^F$ according to our choice, we obtain

$$\begin{aligned} -2\langle B_{h,j}(A_{h,j}^{-1})^*B_{h,j}^*(\boldsymbol{v}_{h,n_j}^F + \eta u_h^F), \boldsymbol{\tau}_{h,n_j}^F + \eta\xi_h^F\rangle_X & \\ -2\langle \boldsymbol{v}_{h,n_j}^F, \boldsymbol{\tau}_{h,n_j}^F\rangle_X + 2\langle\frac{\eta}{q}u_h^F, \eta\xi_h^F\rangle_{X,\Gamma} &= -2\langle\frac{1}{1-Q}P_h\tilde{g}, \eta\xi_h^F\rangle_{X,\Gamma} \\ &= -2\langle\frac{1}{1-Q}g, \eta\xi_h^F\rangle_{X,\Gamma}, \end{aligned}$$

where the last equality holds because η is constant on each facet and which is equivalent to the hybridized problem (19). These steps can be reversed to prove that any solution of the hybridized system gives rise to a solution of the finite element UWVF.

The equivalence of the two methods and an easy link between the variables has thus been established. Since the final solution of both methods is the solution of the Raviart-Thomas method solution this is scarcely surprising, however the direct identification of variables provided in (20) and (23) shows that even the auxiliary variables are linked.

4. Solver strategies

In this section, we propose strategies for solving the equations arising from the discrete UWVF and the hybridized Raviart-Thomas formulation. The finite element UWVF results in a non-symmetric linear system, on which we use a preconditioned GMRES method. On the other hand, the hybridized system is complex symmetric. We observed good convergence behavior of a preconditioned CG method. For the preconditioner, we use a multiplicative Schwarz block preconditioner described in more detail shortly.

For the UWVF, one can also use traces of plane wave functions for the finite element space, as done in [7]. We shall indicate how to couple the finite element UWVF and plane wave UWVF later in this section, thereby exploiting the benefits of both.

4.1. **Solving the UWVF equations.** We first derive a matrix problem corresponding to the discrete finite element UWVF equation (15) by choosing a basis $\{X_{jk} : j \in J_h, k \in I(j)\}$ for the finite element space X_h. For X_{jk} the first index j denotes to which element T_j the basis function is associated, while $k \in I(j)$ is the local degree of freedom on T_j. To obtain a basis for the full trace space $P^p(F)$ on an element facet F, we propose to use Legendre polynomials along the edges in two space dimensions. In the three dimensional case, we construct a polynomial basis for P^p on the triangle using the Duffy transform. For $\mathcal{X}_h \in X_h$ we can determine a unique vector $\vec{X} = (\underline{x}_{jk})$ such that

$$\mathcal{X}_h = \sum_{j \in J_h} \sum_{k \in I(j)} \underline{x}_{jk} X_{jk}.$$

Then we can rewrite problem (15) as the problem of finding $\vec{X}$ such that

$$D_h \vec{X} - C_h \vec{X} = \vec{F}.$$

Here D_h is a block-diagonal, symmetric, positive definite sparse matrix defined by

$$(D_h)_{ij,kl} = \langle X_{kl}, X_{ij} \rangle_X,$$

whereas C_h is given by

$$(C_h)_{ij,kl} = \langle \Pi X_{kl}, F_h(X_{ij}) \rangle_X,$$

and $\vec{F} = (\underline{f}_{ij})$ is the right hand side, $\underline{f}_{ij} = \langle \tilde{g}, F_h(X_{ij}) \rangle_X$.

As suggested in [7], we use the inverse of D_h for preconditioning. As this matrix is block-diagonal, a multiplication by D_h^{-1} can be done in optimal complexity. The preconditioned equation reads

$$(I - D_h^{-1} C_h) \vec{X} = D_h^{-1} \vec{F}. \tag{24}$$

We solve the preconditioned linear system (24) by a GMRES method.

The original papers of Cessenat and Després advocated solving (24) by a damped fixed point iteration. The following lemma ensures convergence of such a method also for the FE-UWVF.

Lemma 10. *Let λ be an eigenvalue of $D_h^{-1} C_h$. For h small enough, it satisfies*

$$|\lambda| \leq 1$$

and $\lambda \neq 1$.

Proof. Clearly, an eigenvalue λ is a generalized eigenvalue for an eigenvector $\vec{X}$,

$$C_h \vec{X} = \lambda D_h \vec{X}.$$

Due to the definitions of the matrices C_h, D_h, this implies

$$\langle F_h^* \Pi \mathcal{X}_h, \mathcal{Y}_h \rangle_X = \lambda \langle \mathcal{X}_h, \mathcal{Y}_h \rangle_X.$$

As F_h is an isometry in X, and $\|\Pi\|_{X \to X} \leq 1$, we see $|\lambda| \leq 1$. The fact that $\lambda = 1$ is excluded follows from the unique solvability of the discrete equation (15). □

4.2. **Solving the hybridized system.** In the same way as for the UWVF equations, we derive a matrix problem corresponding to the hybridized scheme for a specific finite element basis. We choose bases $\{U_i^F\}, \{\boldsymbol{V}_i^F\}$ for U_h^F, V_h^F respectively. This defines a vector representation $\vec{u} = (\underline{u}_i), \vec{\boldsymbol{v}} = (\underline{\boldsymbol{v}}_i)$ of $u_h^F, \boldsymbol{v}_h^F$, such that

$$u_h^F = \sum_i \underline{u}_i U_i^F, \quad \boldsymbol{v}_h^F = \sum_i \underline{\boldsymbol{v}}_i \boldsymbol{V}_i^F.$$

We can rewrite the Schur complement system (19) as

$$S_h(\vec{u}, \vec{\boldsymbol{v}}) = \vec{F}_h,$$

where the matrix and vector entries are given by evaluation of $\mathcal{S}_h$ and the right hand side against basis functions $U_i^F, \boldsymbol{V}_i^F$.

To solve the discrete linear system arising from the hybridized Helmholtz equation, we use a preconditioned CG method. We obtained good convergence results when using an additive Schwarz type block preconditioner. The blocks we use contain all degrees of freedom corresponding to one element. For an element T_i, we define the index set I_{T_i} such that it contains all indices of basis functions corresponding to the facets of element T_i. Let E_i denote the restriction matrix for element T_i, i.e., to the index set I_{T_i}. Then the vector representations $(\vec{u}^F, \vec{\boldsymbol{v}}^F)$ can be decomposed (non-uniquely) into element vectors $\vec{u}_i^F, \vec{\boldsymbol{v}}_i^F$ such that

$$(\vec{u}^F, \vec{\boldsymbol{v}}^F) = \sum_{i \in J_h} E_i^T (\vec{u}_i^F, \vec{\boldsymbol{v}}_i^F).$$

The additive Schwarz preconditioner $\tilde{S}^{-1}$ is applied via

$$\tilde{S}^{-1}(\vec{\xi}_i^F, \vec{\boldsymbol{\tau}}_i^F) = \sum_{i \in J_h} E_i S_i^{-1} E_i^T (\vec{\xi}_i^F, \vec{\boldsymbol{\tau}}_i^F), \qquad S_i = E_i S_h E_i^T.$$

4.3. **Coupling to plane waves.** As proposed by Cessenat and Després [7], we can also discretize the UWVF-space X using impedance traces of plane wave functions. On a plane wave element T_i with boundary ∂T_i, we use the following basis functions X_{ij}

$$\begin{aligned} X_{ij} &:= \Big(\frac{1}{i\kappa}\frac{\partial}{\partial n_i} + \eta\, id\Big) e_{ij}, \\ e_{ij}(x) &:= \exp(i\kappa d_{ij} \cdot x), \quad d_{ij} := (\cos(2j\pi/p_i), \sin(2j\pi/p_i))^T. \end{aligned}$$

As plane wave functions are solutions to the adjoint problem (12), the application of F_h to $\mathcal{X}_{ij}$ on ∂T_i reduces to

$$F_{h,i}(X_{ij}) = \Big(-\frac{1}{i\kappa}\frac{\partial}{\partial n_i} + \eta\, id\Big) e_{ij}.$$

A general rule of thumb (in two dimensions and for high κ) is to choose the order of the finite element basis functions element by element so that on T_i $p_i = ch_i\kappa + 1$, with $c = O(1)$, for both polynomial and plane wave ansatz functions (see [1] for

an analysis of dispersion for high order finite elements on rectangles where this relation is proved).

On large elements, one can save a considerable number of degrees of freedom when using plane wave ansatz functions compared to polynomials. On the other hand, on small elements the plane waves are almost linearly dependent. However, the two different types of finite elements can be coupled in a straightforward way. This way, we can exploit the benefits of both, using plane waves for large elements of high order, and polynomials for those of low order. An example of this technique is shown in Section 5.2.

5. Further Numerical results

In this section, we give some computational results in two and three space dimensions that illustrate the behavior of our hybridization strategies.

5.1. **Propagation in a simple domain.** For our first example, we prescribe the incoming impedance trace $\frac{1}{ik}\frac{\partial u}{\partial n} - u$ on the boundary of a unit square, such that the solution is given by $u = \exp(i\kappa d \cdot x)$, where $d = (\cos(1), \sin(1))$. We discretize the domain by an unstructured triangular mesh containing 904 elements, with mesh size $h = 0.05$. We test both methods for different values of κ. We use polynomial finite element spaces of uniform order $p = 1$ and $p = 3$. In the UWVF, we also use plane-wave elements with 10 directions as discussed in Section 4.3, and a variable-order approach where the order is defined element-wise by $p = 1 + 1.5h\kappa$. Then, we use polynomial elements up to order 4, and plane-wave elements for the higher orders. As discussed in the previous section, we apply a GMRES/CG solver to the respective preconditioned systems.

We compare the convergence of the iterative solvers for the two methods for different wave lengths and mesh sizes. In Table 1, we give the numbers of iterations needed to reduce the error by a factor of 10^{-8}. For $p = 1, \kappa = 80$ the plane wave solution is not resolved by the finite element functions. Then the GMRES method for the ultra-weak equation does not converge within 1000 iterations (for more details on computational aspects of the UWVF see [18]). When damping the hybridized system as described in Section 5.3, we obtain a solution to the discrete equations within approximately 31 iterations. In Figure 1, we plot the discretization error $\|u - u_h\|_{L^2}$ against the number of degrees of freedom for the above problem. We use elements of orders zero or one on an unstructured, globally refined triangular mesh. As expected, we obtain linear or quadratic convergence with respect to the mesh size. In Figure 2, we plot the error versus the wave-number κ for a fixed mesh, again using elements of order 0 or 1. As expected, the error increases with κ (as a result of dispersion error) even though the number of iterations needed to obtain the solution is almost independent of κ (see Table 1). When we use $p = 1 + h\kappa$ in our calculations, we see that the dispersion error is controlled, and the global L^2 error does not increase when κ is growing.

	UWVF				hybrid	
κ	$p=1$	$p=3$	$p=10$	var. p	$p=1$	$p=3$
5	405	547	589	403	49	51
10	368	485	461	364	49	49
20	343	406	363	380	43	41
40	315	377	316	385	39	39
80	—	359	325	295	–	37

TABLE 1. Number of iterations in GMRES/CG method when approximating the problem discussed in Section 5.1.

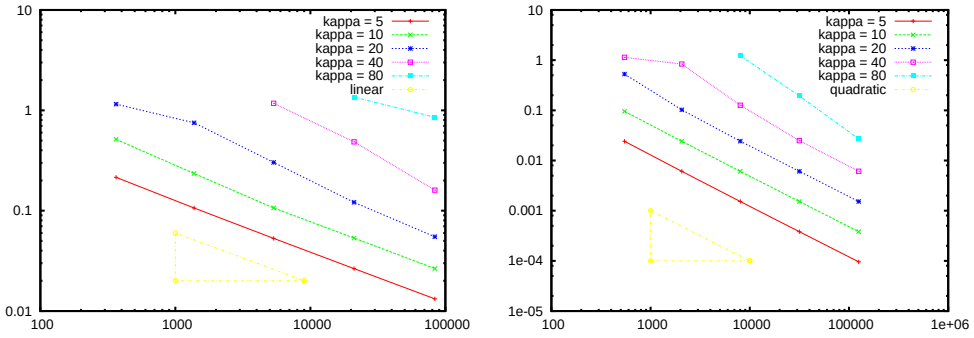

FIGURE 1. Error $\|u-u_h\|_{L^2}$ versus the number of degrees of freedom for the problem in Section 5.1: left $p=0$, right $p=1$. As expected we obtain first order accuracy when $p=0$ and second order when $p=1$, and the error increases with wave-number κ.

In [1] it was shown, that on rectangular, tensor product elements the primal p-version finite element method converges as $(\kappa he/(2(2p+1)))^{2p+1}$. Now, we choose κ in the above problem such that $\kappa he/(2(2p+1)) = c$ for a polynomial degree p varying from one to 16. We choose the constant $c \in [0.5, 1.5]$, and plot the respective error curves in Figure 3. For c small enough, we observe the expected exponential convergence.

5.2. **Coupling the finite element and plane wave UWVF.** We compute the solution of the Helmholtz equation on a 2D L-shaped domain with wave-number $\kappa = 100$ as shown in Figure 4. We assume a Dirichlet condition on the inner boundary part of the L-shape, and a transparent boundary condition everywhere else. At the corner point, a singularity of the solution occurs. We use a triangular mesh of mesh size 0.3, and a geometric refinement towards the reentrant corner. On each element, we compute its order by $p = ch\kappa + 1$ for $c \simeq 1$. This way we get the number of degrees of freedom per wavelength, which was observed to be necessary to resolve the wave-like character of the solution. A reference solution

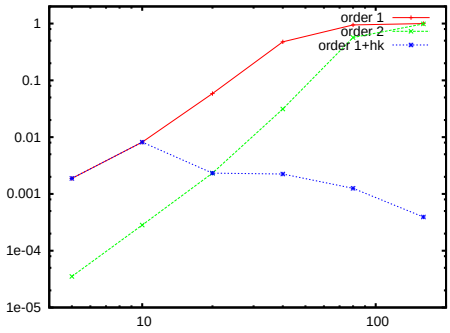

FIGURE 2. Error $\|u - u_h\|_{L^2}$ versus wave-number κ when $p = 0$ (333,056 dofs), and $p = 1$: (499,584 dofs). As expected the error increases with κ, even though the number of GMRES/CG iterations is essentially independent of κ (see Table 1). For $p = 1 + h\kappa$, the error even decreases slightly.

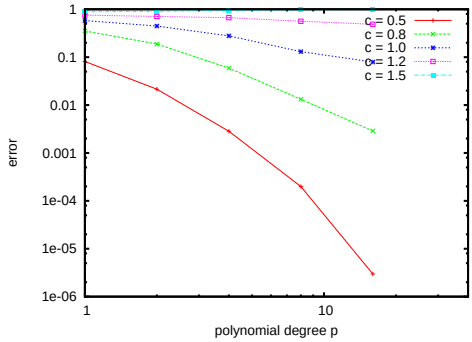

FIGURE 3. Error $\|u - u_h\|_{L^2}$ versus polynomial degree p, wave number κ such that $\kappa he/(2(2p + 1)) = c$. We see the exponential convergence for c small enough.

can be computed using high order standard Raviart-Thomas elements and mesh refinement. This is shown in the top row of pictures in Figure 4. A blowup of the solution near the reentrant corner shows why mesh refinement is needed.

In the middle row of pictures we use a typical plane wave UWVF grid without mesh refinement towards the singularity. Clearly the solution near the singularity is not well approximated. If the mesh is refined towards the singularity, the plane wave UWVF can approximate the solution (see for example [17]), but there is no advantage to plane wave bases on small elements, so we instead polynomial elements for those elements where the order is small (i.e. h_i is small), and plane-wave elements everywhere else. For our example, the orders varied between one and fifty, we obtained a total of only 4463 face-based degrees of freedom. In the bottom row of Figure 4, we display the solution u and the absolute value of

the gradient in the vicinity of the singular point with this combined approach. When using polynomial elements only, we needed far more memory resources. To obtain a solution of similar accuracy as for the coupled approach, we used a finer mesh ($h \simeq 0.1$), and elements of polynomial order up to 6, which resulted in 37832 coupling degrees of freedom.

5.3. **Damping of unresolved waves.** Due to the oscillatory behavior of solutions to the Helmholtz equation, a sufficiently large number of degrees of freedom per wavelength is necessary to resolve the solution (at least π for a very high order finite element method [1]). As the wave number κ increases, it may not be possible to perform the calculations with sufficient accuracy due to hardware and/or time limitations. Then a method, where unresolved components of the solution are damped, is desirable. Due to the fact that the UWVF-operator F_h is an isometry from the trace space X_h into itself, the original method does not provide such a damping effect.

For the facet-based hybridization, we obtain a damping scheme, when adding a consistent stabilization term

$$\begin{aligned}&\mathcal{B}_h^S(u_h, \boldsymbol{v}_h, u_h^F, \boldsymbol{v}_h^F; \xi_h, \boldsymbol{\tau}_h, \xi_h^F, \boldsymbol{\tau}_h^F) := \\ &\qquad \mathcal{B}_h(u_h, \boldsymbol{v}_h, u_h^F, \boldsymbol{v}_h^F; \xi_h, \boldsymbol{\tau}_h, \xi_h^F, \boldsymbol{\tau}_h^F) - \sum_{j \in J_h} (\eta(u_h - u_h^F), \xi_h - \xi_h^F)_{\partial T_j}.\end{aligned} \tag{25}$$

This method can be useful, when a good approximation of the solution is only needed locally on a small portion of the underlying domain, and no accuracy is necessary in the remaining part. As an example, we use a circular domain Ω of radius one, where we have some incoming impedance trace prescribed on a concentric circular hole of radius 0.05. On the outside, we assume absorbing boundary conditions. Now, we divide this ring into two parts Ω_1, Ω_2 by a further concentric circle of radius 0.3. We use a mesh which has maximum mesh size $h_1 = 0.05$ in the inner part Ω_1, and mesh size $h_2 = 0.25$ in the outer part Ω_2. This mesh consists of 892 triangular elements. We calculate the solution, using Raviart-Thomas elements of orders one to four. Then, the wave is sufficiently well resolved on the inner part, but not on the outer ring. We calculate the error arising on the inner ring, $\|u - u_h\|_{\Omega_1}$, using both the original and the damping method. In Table 2, we see that the results are much better for the damping scheme. In this case, also the CG method converges faster. In Figure 5, we plot the solution u_h and its absolute value $|u_h|$ for both schemes, using order $p = 3$. One can see the better quality of the solution when the damping term is added.

5.4. **A three dimensional example.** As an example in three space dimensions, we consider an object enclosed in the unit sphere. The wave number is set to $\kappa = 40$. On a small part of the boundary, we assume a source generated by an inhomogeneous Dirichlet condition. The rest of the boundary is governed by an absorbing boundary condition. We observe the field scattered on the object. We

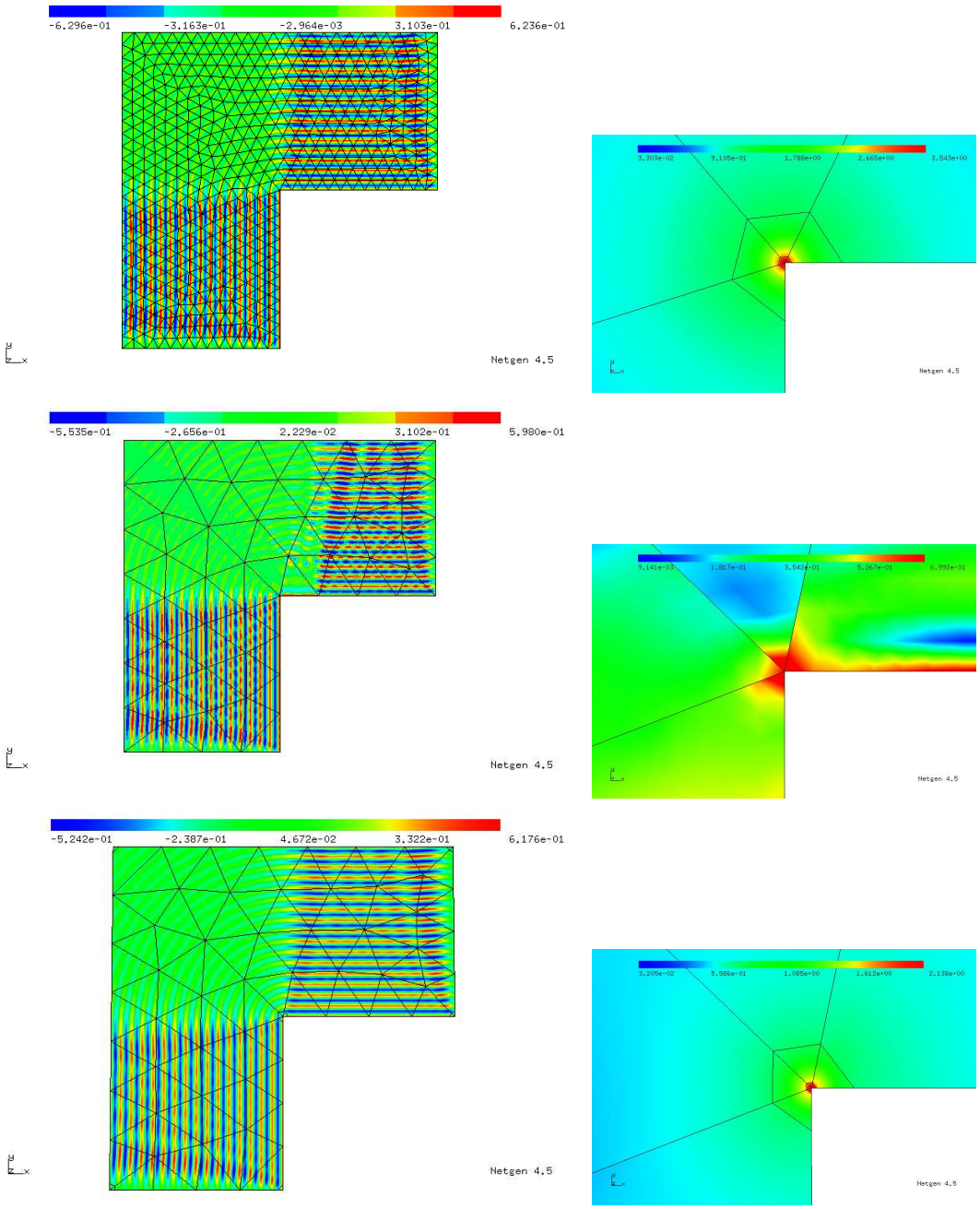

FIGURE 4. Results for the L-shaped domain. In the top row we show a reference solution computed using variable order Raviart-Thomas elements. In the middle row we show the traditional plane wave UWVF solution on an unrefined grid. Grid refinement is necessary for the UWVF to obtain accuracy and in the bottom row we show the solution computed using the plane wave UWVF on large elements, and low order Raviart-Thomas functions on small elements. Left: solution u, right: $|\boldsymbol{v}|$ around singularity.

		error (CG-it.)	
p	dofs	damping	original
1	5424	0.19005 (33)	0.275907 (58)
2	8136	0.0627521 (90)	0.176839 (114)
3	10848	0.0528101 (103)	0.193589 (125)
4	13560	0.0473072 (103)	0.157117 (129)

TABLE 2. Here we show the effect of adding the damping term in (25) when the wave is under-resolved in a part of the domain Ω_2. We compare the error $\|u - u_h\|_{\Omega_1}$ on the remaining part, and give the number of CG iterations needed for an error reduction of 10^{-10}.

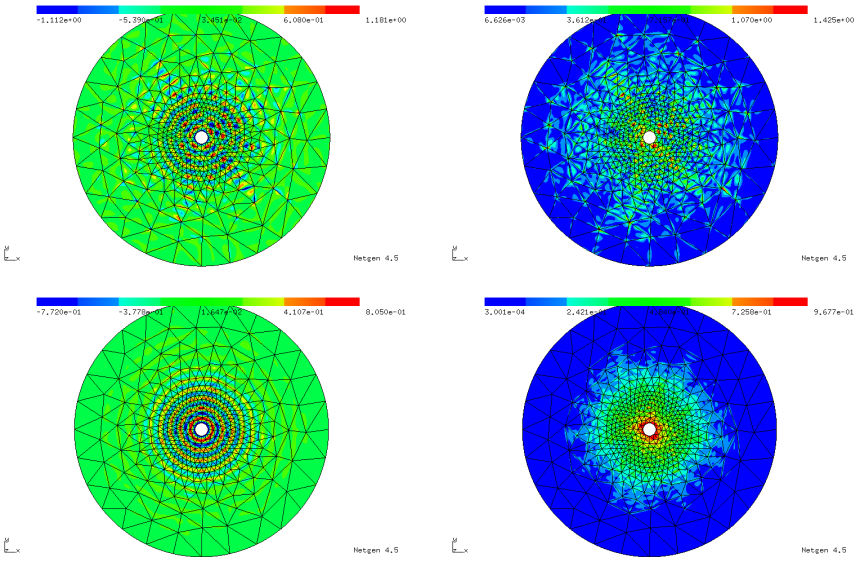

FIGURE 5. Here we show the effect of adding the damping term in (25) when the wave is under-resolved (i.e. an insufficient number of unknowns per wavelength). In the top row we show our original hybridization scheme with no damping (left: u, right : $|u|$). In the bottom row we show the corresponding results with damping added. When the damping term is included the iterative scheme converges more rapidly.

expect singularities of the solution on the reentrant edges arising at edges of the object. We do a two-level geometric mesh refinement towards these parts. We apply the facet-based hybridization method. We solve on a mesh consisting of a hybrid mesh of 14082 elements, using RT_5/P^5 elements. This leads to 5828748 degrees of freedom, 1315956 of which are facet-based. We need 204 iterations

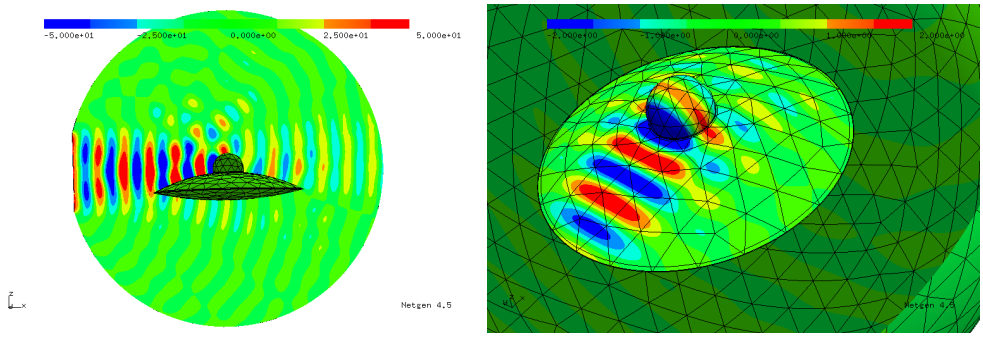

FIGURE 6. Solution u_h in the interior (right), trace u_h^F on the boundary

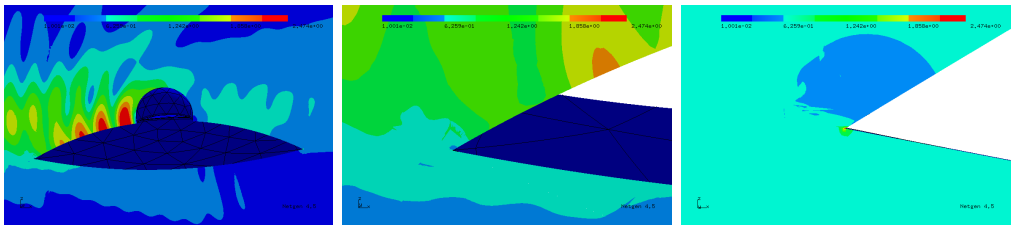

FIGURE 7. Absolute value of flux $|\boldsymbol{v}_h|$, zoom to singularity

to reach an error reduction of 10^{-10}. Figure 6 shows the scalar field u_h in the interior and its trace u_h^F on the object. In Figure 7, we plot the absolute value of the flux, zooming to the singularity.

6. Conclusion

We have presented two methods for solving the Helmholtz equation with a large wave number κ. One is an Ultra Weak Variational Formulation, the other one stems from a hybridization approach similar to those developed for Laplace's equation. Both methods are based on a mixed formulation of the problem, and using Raviart-Thomas finite elements. We showed that the two schemes are equivalent up to a change of variables.

In our numerical examples, we saw that the approximation properties for both the h and p version of the finite element method are as expected. We obtain optimal algebraic convergence when doing uniform mesh refinement. When increasing p proportional to κ, we see the expected exponential convergence.

We solve both systems by iterative methods, namely a preconditioned GMRES method for the UWVF, and a preconditioned CG method for the hybridized equations. In the first case, we used a mass matrix as a preconditioner, as originally proposed by Cessenat and Déspres. For the hybridized equations, we propose an additive Schwarz block preconditioner. In both cases, we observe that the number of iterations is independent of κ. However, the iteration counts obtained

for the second scheme were much smaller than for the first, presumably due to a better preconditioner.

In the UWVF approach, the Raviart-Thomas based method can be easily coupled to an UWVF using plane waves. This can be useful when singularities in the solution are to be resolved by geometric grid refinement: By using polynomials/plane waves on small/large elements, serious ill-conditioning of the matrix is avoided, while a huge number of degrees of freedom can be saved.

References

[1] M. Ainsworth. Discrete dispersion relation for *hp*-version finite element approximation at high wave number. *SIAM J. Numer. Anal.*, 42(2):553–575, 2004.

[2] D. N. Arnold and F. Brezzi. Mixed and nonconforming finite element methods: implementation, postprocessing and error estimates. *RAIRO Model. Math. Anal. Numer.*, 19:7–32, 1985.

[3] I. Babuška and J. Melenk. The Partition of unity method. *Int. J. Numer. Methods Eng.*, 40:727–758, 1997.

[4] D. Boffi, F. Brezzi, and L. Gastaldi. On the problem of spurious eigenvalues in the approximation of linear elliptic problems in mixed form. *Math. Comput.*, 69:121–40, 2000.

[5] F. Brezzi and M. Fortin. *Mixed and Hybrid Finite Element Methods*. Springer, New York, 1991.

[6] O. Cessenat. *Application d'une nouvelle formulation variationnelle aux équations d'ondes harmoniques. Problèmes de Helmholtz 2D et de Maxwell 3D.* PhD thesis, Université Paris IX Dauphine, 1996.

[7] O. Cessenat and B. Després. Application of an ultra weak variational formulation of elliptic PDEs to the two-dimensional Helmholtz problem. *SIAM J. Numer. Anal.*, 35:255–299, 1998.

[8] O. Cessenat and B. Després. Using plane waves as base functions for solving time harmonic equations with the ultra weak variational formulation. *J. Computational Acoustics*, 11:227–238, 2003.

[9] B. Cockburn, J. Gopalakrishnan, and R. Lazarov. Unified hybridization of discontinuous Galerkin, mixed and conforming Galerkin methods for second order elliptic problems. *preprint*, 2007.

[10] L. Demkowicz, P. Monk, and L. Vardapetyan. de Rham diagram for *hp* finite element spaces. *Comput. Math. Appl.*, 39:29–38, 2000.

[11] B. Després. Sur une formulation variationelle de type ultra-faible. *C.R. Acad. Sci. Paris, Ser. I*, 318:939–944, 1994.

[12] Y. Erlangga, C. Oosterlee, and C. Vuik. A novel multigrid based preconditioner for heterogeneous Helmholtz problems. *SIAM J. Sci. Comp.*, 27:1471–92, 2006.

[13] C. Farhat, I. Harari and U. Hetmaniuk. A discontinuous Galerkin method with Lagrange multipliers for the solution of Helmholtz problems in the mid-frequency regime. *Computer Methods in Applied Mechanics and Engineering*, 192:1389–1419, 2003.

[14] C. Farhat, R. Tezaur and P. Weidemann-Goiran. Higher-order extensions of a discontinuous Galerkin method for mid-frequency Helmholtz problems. *Int. J. Numer. Meth. Engr.*, 61:1938 – 1956, 2004.

[15] V. Girault and P. A. Raviart. *Finite Element Methods for Navier-Stokes Equations*. Springer-Verlag, Berlin Heidelberg New York Tokyo, 1986.

[16] C. J. Gittelson, R. Hiptmair, I. Perugia. Plane wave discontinuous Galerkin methods. *Isaac Newton Institute Preprint Series*, 2007.

[17] T. Huttunen, P. Gamallo, and R. Astley. Comparison of two wave element methods for the Helmholtz problem. *Communications in Numerical Methods in Engineering*, 2008.
[18] T. Huttunen, P. Monk, and J. Kaipio. Computational aspects of the Ultra Weak Variational Formulation. *Journal of Computational Physics*, 182:27–46, 2002.
[19] F. Ihlenburg. *Finite Element Analysis of Acoustic Scattering*, volume 132 of *Applied Mathematical Sciences*. Springer, Berlin, 1998.
[20] M. Melenk. *On Generalized Finite Element Methods*. PhD thesis, University of Maryland, U.S., 1995.
[21] P. Monk. *Finite Element Methods for Maxwell's Equations*. Oxford University Press, Oxford, 2003.
[22] J. C. Nédélec. Mixed finite elements in $\mathbb{R}^3$. *Numer. Math.*, 35:315–341, 1980.
[23] E. Perrey-Debain, O. Laghrouche, P. Bettess and J. Trevelyan. Plane-wave basis finite elements and boundary elements for three-dimensional wave scattering. *Royal Society of London Philosophical Transactions Series A*, 362:561–577, Mar. 2004.
[24] P. A. Raviart and J. M. Thomas. A mixed finite element method for 2nd order elliptic problems. In *Mathematical Aspects of the Finite Element Method, Lecture Notes in Mathematics*, volume 606, pages 292–315. Springer-Verlag, New York, 1977.